Using One-Dimensional Radiosity to Model Neutral Particle Flux in High Aspect Ratio Holes

Paul Manstetten*, Lado Filipovic†, Andreas Hössinger‡, Josef Weinbub*, and Siegfried Selberherr†
*Christian Doppler Laboratory for High Performance TCAD at the
†Institute for Microelectronics, TU Wien, Gußhausstraße 27-29/E360, 1040 Wien, Austria
‡Silvaco Europe Ltd., Compass Point, St Ives, Cambridge, PE27 5JL, United Kingdom
Email: manstetten@iue.tuwien.ac.at

***Abstract*—We present a computationally inexpensive one-dimensional method to model the neutral flux in high aspect ratio holes for three-dimensional plasma etching simulations. The benefit of our approach lies in the fact that the computational costs of a three-dimensional plasma etching simulation are, for the most part, determined by calculating the surface flux of the relevant species. We propose a one-dimensional radiosity model for the neutral flux by assuming an ideal cylindrical shape as well as ideal diffuse sources and surfaces. Our model reproduces the results obtained by a three-dimensional ray tracing simulation and is therefore suited to be used as a drop-in replacement for cylinder-like hole structures to speed up three-dimensional plasma etching simulations.**

I. Introduction

During a plasma etching simulation the local fluxes of the etching species are used to model the surface reactions. The local flux must be recalculated for each simulation time step, because the interface positions are changing due to the evolving surface. For high aspect ratio (HAR) features, the local flux originating from re-emission is predominant and the local flux rates can easily vary by orders of magnitude along the feature depth.

Considering the computational costs of a three-dimensional plasma etching simulation, the calculation of the local flux is dominant. The efficient calculation of the neutral flux is therefore essential, especially considering the fact that HARs further increase this dominance, because with a high aspect ratio the average number of re-emission events per particle is also increased.

Common approaches for three-dimensional flux calculation are Monte Carlo ray tracing [1] and radiosity based [2] methods. Ray tracing supports bi-directional reflectance distribution functions, whereas radiosity inherently favors diffusely reflecting surfaces. The rotational symmetry allows to use a one-dimensional radiosity method which is intended to be a drop-in replacement for modeling the neutral flux in cylinder-like hole structures in three-dimensional simulations, with the benefit of decreased computational complexity.

In this work we consider an ideal cylindrical shape of the feature, a neutral flux source with an isotropic distribution, ideal diffuse reflections, and a flux-independent sticking probability s. Ballistic transport is assumed for the neutral particles. The diffuse re-emission mechanism is a common assumption for neutral particles [3] and cylinder-like shapes are a key prerequisite for HAR holes in the context of, for instance, three-dimensional NAND flash cell processing [4].

In the following sections, we first define our simulation domain with all relevant parameters (II-A) and explain the applied discretization (II-B); subsequently we describe how to adopt the general radiosity method to our problem (II-C) and how we compute the relevant view factors (II-D). We apply the Jacobi method to solve the resulting linear system of equations (II-E) and apply a normalization to the resulting flux distributions (II-F). Finally, we discuss the results (III) of our model and compare them with results obtained using a three-dimensional ray tracing simulation [5].

II. One-Dimensional Radiosity for Cylindrical Holes

A. Simulation Domain

The simulation domain (Fig. 1a) is a circular cylinder with its aspect ratio (AR) defined by $\frac{\text{depth}}{\text{diameter}}$. We model the source of neutral particles by an ideal diffusely-emitting disk closing the cylinder at the top without re-emission ($s = 1$). The wall of the cylinder is an ideal diffuse reflector with a constant sticking probability ($s = s_w$). The bottom of the cylinder does not have any re-emission ($s = 1$). This setup is a reasonable approximation for the neutral flux in a HAR plasma etching environment.

B. Domain Discretization

Our approach is based on a subdivision of the cylinder into rotationally symmetric surface elements (Fig. 1b): The inner surface of the cylinder wall is sliced into n_w cylinder rings with height $\frac{\text{depth}}{n_w}$ and the disk closing the cylinder at the bottom is divided into n_b annuli with ring width $\frac{\text{radius}}{n_b}$. The disk closing the cylinder at the top is not subdivided, as it is fully adsorbing and the distribution of the flux leaving the cylinder at the top is not of interest.

C. Applying the Radiosity Method

Our assumptions, particularly that all sources/surfaces are ideal diffuse and that the transport of the neutral particles is ballistic, allows to employ the radiosity method. By assuming a constant flux and a constant sticking probability over each surface element, the problem can be formulated using the

ISBN 978-1-4673-8608-1 IEEE Catalog number CFP1649D-USB

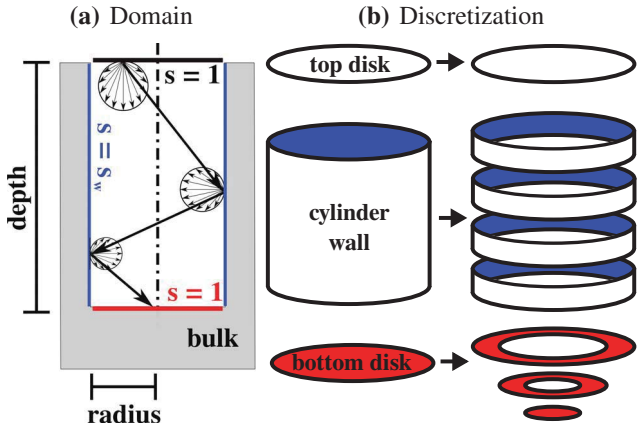

Fig. 1. (a) The simulation domain is decomposed into a fully adsorbing source (black), a partly adsorbing wall (blue), and a fully adsorbing bottom (red). (b) The wall and bottom are subdivided into ring elements. The top disk is not subdivided as the flux distribution leaving the cylinder is irrelevant.

discrete radiosity equation: for a surface element i the equation reads

$$B_i = E_i + (1 - \alpha_i) \sum_j (F_{j \to i} B_j), \tag{1}$$

where B is the radiosity (sum of emitted and reflected energy), E is the emitted energy, α is the absorptance and $F_{j \to i}$ is the view factor (proportion of the radiated energy which leaves element j and is received by element i). We adapt (1) to our problem by substituting the absorptance α by the sticking probability s and identifying the local flux as the adsorbed energy A. The radiosity B is then related to the adsorbed energy A by

$$A_i = (B_i - E_i) \frac{s_i}{1 - s_i}. \tag{2}$$

Since we are also interested in the adsorbed flux at the fully adsorbing bottom, (1) and (2) are not applicable because $\lim_{s_i \to 1} A_i = \infty$. For this reason we use the following formulation for the received energy R:

$$R_i = \sum_j (E_j F_{j \to i}) + \sum_j ((1 - s_j) R_j F_{j \to i}), \tag{3}$$

where the relation to the adsorbed energy is

$$A_i = R_i s_i. \tag{4}$$

Rewritten in matrix notation and resolved for the vector of received energies R we obtain

$$\begin{aligned} \mathbf{F}^T \cdot E + \operatorname{diag}(1 - \mathbf{s})\, \mathbf{F}^T \cdot R &= R, \\ \left(\mathbf{I} - \operatorname{diag}(1 - \mathbf{s})\, \mathbf{F}^T\right) \cdot R &= \mathbf{F}^T \cdot E, \end{aligned} \tag{5}$$

with vectors of source energies E, a vector of sticking probabilities $\mathbf{s}$, and a matrix of view factors $\mathbf{F}$ (where entry F_{ij} is the view factor from $i \to j$).

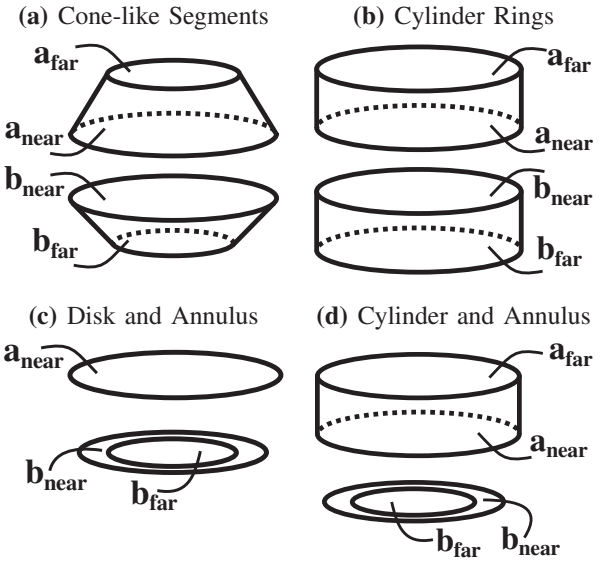

Fig. 2. (a) Configuration of two cone-like segments opened towards each other. The inner surfaces are mutually completely visible. (b) Configuration of two coaxial cylinder rings with the same radius. (c) Configuration of a disk and an annulus. (d) Configuration of a cylinder element and a annulus. The outer radius of the annulus is not greater than the cylinder radius.

D. Computing the View Factors

To assemble the matrix $\mathbf{F}$ we need to evaluate the view factors between all possible pairs of surface elements. The view factor between two coaxial disks at a distance z of unequal radii r_1 and r_2 is defined by

$$F_{1 \to 2} = \frac{1}{2} \left(X - \sqrt{X^2 - 4(R_1/R_2)^2} \right), \tag{6}$$

where $R_i = r_i/z$ and $X = 1 + (1 + R_2^2)/R_1^2$ [6]. Using this relation and the reciprocity theorem of view factors

$$S_1 \cdot F_{1 \to 2} = S_2 \cdot F_{2 \to 1} \quad (\text{with } S_i = Area_i), \tag{7}$$

we derive a general formula for a view factor between two cone-like segments whose surfaces are mutually completely visible.

$$F_{b_x \to a} = F_{b_x \to a_{near}} - F_{b_x \to a_{far}} \tag{8}$$

$$F_{a \to b_x} = \frac{S_{b_x}}{S_a} \cdot F_{b_x \to a} \tag{9}$$

$$F_{a \to b} = F_{a \to b_{near}} - F_{a \to b_{far}} \tag{10}$$

Fig. 2a shows the geometric configuration of two cone-like segments opened towards each other with mutually completely visible surfaces; the four limiting disks which enter Eqs. (8)-(10) are designated. Fig. 2b, Fig. 2d and Fig. 2c show the main types of configurations as they occur in our problem.

The view factors on the diagonal of $\mathbf{F}$ (i.e., the view factors of the elements to themselves) are computed by

$$F_{a \to a} = 1 - F_{a \to a_{near}} - F_{a \to a_{far}}. \tag{11}$$

If the element is a disk or annulus, the view factor to itself is zero.

To reduce the computational costs for assembling $\mathbf{F}$ we can make use of the fact that the cylinder rings are regular and the $(n_w)^2$ view factors amongst them can be affiliated with only n_w different view factors, as only the relative distance matters. Reciprocity (7) allows the computation of the view factors in the upper triangle of $\mathbf{F}$ by using the view factors in the lower triangle and the element areas.

To prove a closed domain and as indicator for correctly computed view factors we compute the sum for each row of $\mathbf{F}$, which must always result in one.

E. Solving the Linear System of Equations

We approximate the solution of the resulting diagonally-dominant linear system of equations (5) using the Jacobi method. Each iteration of the Jacobi method can be imagined as a concurrent diffuse re-emission of each element to all other elements. The adsorbed flux A is obtained by multiplying the entries in the solution for R with the corresponding sticking probability s of the element (4). To reveal computational mistakes and to have an indicator for an equilibrium state the relation $\| A \| - \| E \| = 0$ can be applied; it holds for closed surfaces, e.g., our domain (the inner surface of a cylinder closed with two disks at the top and bottom).

F. Normalization

To provide a good qualitative comparability we normalize the results to only depend on the aspect ratio of the hole and the sticking probability. The adsorbed flux A is divided by the area of the element ($A_i^n = \frac{A_i}{S_i}$) and normalized to the flux which a surface of the same sticking probability would absorb if it is fully planar-exposed to the source ($A_i^{n_{src}} = \frac{A_i^n}{E_{i_{src}}^n \cdot s_i}$).

III. Results

To evaluate the quality of our one-dimensional radiosity model, we analyze different simulation setups where we vary the sticking probability between $s_w = 0.02$ and $s_w = 0.2$; the top disk (source) and bottom disk are fully adsorbing for all of the following results.

Fig. 3 plots the normalized flux distribution along the wall and the at bottom for holes with ARs 5 and 45. The results show that the flux along the wall of a HAR hole decreases by several orders of magnitude, e.g., about five orders for AR=45 and one order for AR=5. The non-continuity of the sticking probability causes a jump at the wall-bottom interface. The effect of the fully adsorbing bottom is also visible in the wall flux distribution, which is most prominent for $AR = 45$ and $s = 0.02$, where a strong decrease towards the bottom interface is visible.

Fig. 4 compares the flux distributions for $AR = 5$ obtained using the proposed one-dimensional radiosity approach with results generated with a reference Monte Carlo ray tracing tool [5]. Similarly, Fig. 5 compares the flux distributions for $AR = 45$. The results show a good agreement, besides the deviation at the wall-bottom interface, caused by the discretization which is used in the ray tracing simulation. In Fig. 5a two flux distributions are plotted for the ray tracing results along the wall: they represent the minimum and maximum along the cylinder radius. The separation of the flux distributions, particularly visible for $s_w = 0.2$ (Fig. 5a), and the visible noise in Fig. 5b, reflect the stochastic nature of the ray tracing approach.

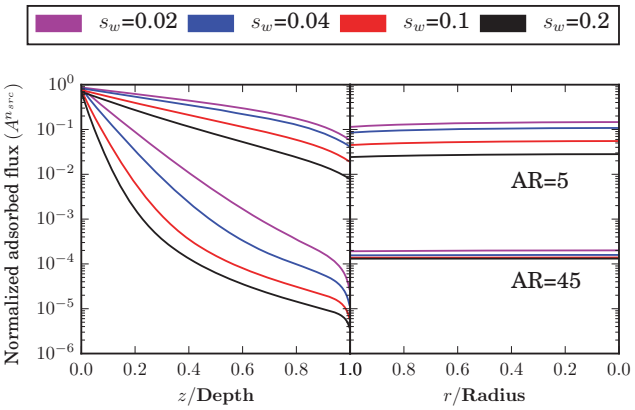

Fig. 3. Normalized flux distribution along the wall (left) and the bottom (right) of holes with aspect ratios AR=5 (upper group) and AR=45 (lower group). The sticking probability of the wall s_w is varied from 0.02 to 0.2.

IV. Summary and Outlook

We provide an approximation of the local neutral flux in three-dimensional plasma etching simulations of HAR holes using a one-dimensional radiosity approach. A radiosity formulation from a receiving perspective (3) is derived, which allows to model fully adsorbing surface elements. We compute all relevant view factors by establishing a general formula (10) between coaxial cone-like segments. Comparing the results for cylinders with ARs 5 and 45 using a rigorous three-dimensional Monte Carlo ray tracing simulation shows good agreement (Fig. 4a and Fig. 5b). Our radiosity model thus serves as a computationally inexpensive drop-in replacement for three-dimensional simulations.

Our approach allows for an extension of the model to handle any rotationally symmetric convex features.

Acknowledgment

The financial support by the *Austrian Federal Ministry of Science, Research and Economy* and the *National Foundation for Research, Technology and Development* is gratefully acknowledged.

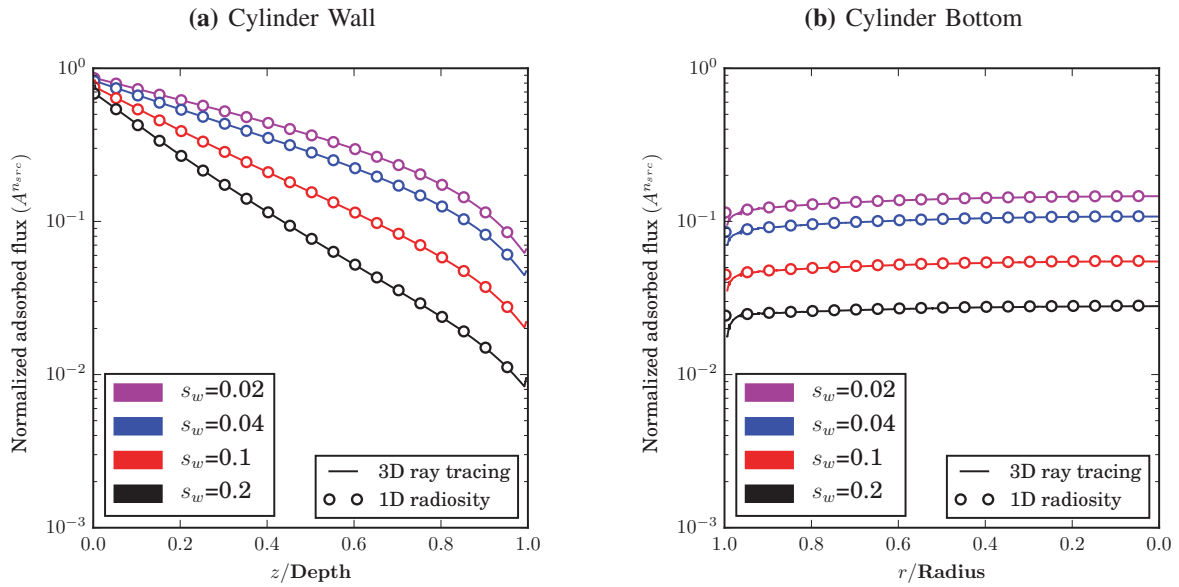

Fig. 4. Comparison of the results obtained by one-dimensional radiosity and three-dimensional raytracing for a hole with aspect ratio 5. The sticking probability of the wall s_w is varied between 0.02 and 0.2. The differences are visible near the wall-bottom interface. (a) Normalized flux distribution along the wall. (b) Normalized flux distribution at the bottom.

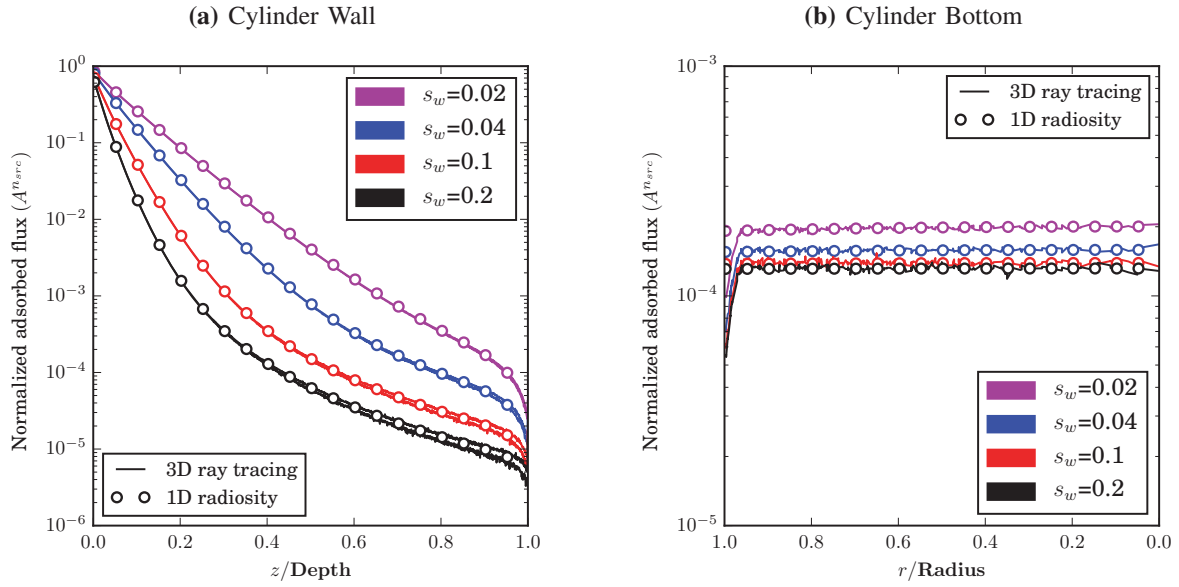

Fig. 5. Comparison of results obtained by one-dimensional radiosity and three-dimensional raytracing for a hole with aspect ratio 45. The sticking probability of the wall s_w is varied between 0.02 and 0.2. The differences are visible near the wall-bottom interface. The ray tracing results reveal noise over the entire domain. (a) Normalized flux distribution along the wall. Along the depth, the minimum and maximum ray tracing results are plotted; the difference increases towards the bottom interface. (b) Normalized flux along the bottom.

References

[1] O. Ertl and S. Selberherr, "Three-Dimensional Level Set Based Bosch Process Simulations Using Ray Tracing for Flux Calculation," *Microelectronic Engineering*, vol. 87, no. 1, pp. 20–29, 2010.

[2] T. Ikeda, H. Saito, F. Kawai, K. Hamada, T. Ohmine, H. Takada, and V. Deshpande, "Development of SF_6/O_2/Si Plasma Etching Topography Simulation Model Using New Flux Estimation Method," in *Proceedings of the 2011 International Conference on Simulation of Semiconductor Processes and Devices (SISPAD)*, 2011, pp. 115–118.

[3] G. Kokkoris, A. G. Boudouvis, and E. Gogolides, "Integrated Framework for the Flux Calculation of Neutral Species Inside Trenches and Holes During Plasma Etching," *Journal of Vacuum Science & Technology A*, vol. 24, no. 6, pp. 2008–2020, 2006.

[4] P. Dimitrakis, *Charge-Trapping Non-Volatile Memories: Volume 1 – Basic and Advanced Devices*. Springer, 2015.

[5] O. Ertl, L. Filipovic, and J. Weinbub, "ViennaTS," https://github.com/viennats/viennats-dev, 2015.

[6] M. F. Modest, *Radiative Heat Transfer*. Academic Press, 2013.